Since January 2020 Elsevier has created a COVID-19 resource centre with free information in English and Mandarin on the novel coronavirus COVID-19. The COVID-19 resource centre is hosted on Elsevier Connect, the company's public news and information website.

Antiviral Research 200 (2022) 105290

Contents lists available at ScienceDirect

Antiviral Research

journal homepage: www.elsevier.com/locate/antiviral

Neutralization or enhancement of SARS-CoV-2 infection by a monoclonal antibody targeting a specific epitope in the spike receptor-binding domain

Guan-Chun Lai [a,1], Tai-Ling Chao [b,c,1], Shiau-Yu Lin [a,1], Han-Chieh Kao [b], Ya-Min Tsai [b], De-Chao Lu [a], Yi-Wei Chiang [a], Sui-Yuan Chang [b,d,**], Shih-Chung Chang [a,e,*]

[a] Department of Biochemical Science and Technology, College of Life Science, National Taiwan University, Taipei, 106, Taiwan
[b] Department of Clinical Laboratory Sciences and Medical Biotechnology, College of Medicine, National Taiwan University, Taipei, 106, Taiwan
[c] Genomics Research Center, Academia Sinica, Taipei, 115, Taiwan
[d] Department of Laboratory Medicine, National Taiwan University Hospital, College of Medicine, National Taiwan University, Taipei, 106, Taiwan
[e] Center of Biotechnology, National Taiwan University, Taipei, 106, Taiwan

ARTICLE INFO

Keywords:
COVID-19
SARS-CoV-2
Neutralizing antibody
Spike receptor binding domain
ACE2
Antibody-dependent enhancement

ABSTRACT

Neutralizing antibodies (NAbs) are believed to be promising prophylactic and therapeutic treatment against the coronavirus disease 2019 (COVID-19), which is caused by severe acute respiratory syndrome coronavirus 2 (SARS-CoV-2). Here, we reported two mouse monoclonal antibodies 7 Eb-4G and 1Ba–3H that specifically recognized the receptor-binding domain (RBD) of SARS-CoV-2 spike (S) protein without exhibiting cross-reactivity with the S proteins of SARS-CoV and MERS-CoV. The binding epitopes of 7 Eb-4G and 1Ba–3H were respectively located in the regions of residues 457–476 and 477–496 in the S protein. Only 1Ba–3H exhibited the neutralizing activity for preventing the pseudotyped lentivirus from binding to the angiotensin-converting enzyme 2 (ACE2)-transfected HEK293T cells. The competitive ELISA further showed that 1Ba–3H interfered with the binding between RBD and ACE2. Epitope mapping experiments demonstrated that a single alanine replacement at residues 480, 482, 484, 485, and 488–491 in the RBD abrogated 1Ba–3H binding. 1Ba–3H exhibited the neutralizing activity against the wild-type, Alpha, Delta, and Epsilon variants of SARS-CoV-2, but lost the neutralizing activity against Gamma variant in the plaque reduction assay. On the contrary, 1Ba–3H enhanced the cellular infection of Gamma variant in a dose-dependent manner. Our findings suggest that the antibody-dependent enhancement of infection mediated by the RBD-specific antibody for different SARS-CoV-2 variants must be considered while developing the NAb.

1. Introduction

Coronavirus disease 2019 (COVID-19) caused by the infection of severe acute respiratory syndrome coronavirus 2 (SARS-CoV-2) has become a pandemic worldwide. SARS-CoV-2 belongs to the betacoronavirus genus, which includes five pathogens that infect humans (Lu et al., 2020; Zheng, 2020). As with other coronaviruses, the spike (S) protein homotrimer on the surface of SARS-CoV-2 plays an essential role in receptor binding and cell entry through a virus-cell membrane fusion mechanism (Huang et al., 2020). The S protein is mainly composed of the N-terminal S1 and the C-terminal S2 domains, with the receptor-binding domain (RBD) located within the S1 domain (Tai et al., 2020). Previous studies have demonstrated that the RBDs of SARS-CoV and SARS-CoV-2 S proteins bind to the same human receptor, angiotensin-converting enzyme 2 (ACE2), for virus entry (Hoffmann et al., 2020; Lan et al., 2020; Shang et al., 2020; Wang et al., 2020b; Yan et al., 2020). The crystal structure of the binding complex of RBD and ACE2 further reveals that several critical amino acid residues within a region called receptor-binding motif (RBM) at the C-terminus of RBD are cooperatively involved in interaction with ACE2 (Kim et al., 2021; Yi et al., 2020). Therefore, RBD is considered as a primary target and an ideal immunogen for drug and vaccine development. In fact, numerous

* Corresponding author. Department of Biochemical Science and Technology, College of Life Science, National Taiwan University, Taipei, 106, Taiwan.
** Corresponding author. Department of Clinical Laboratory Sciences and Medical Biotechnology, College of Medicine, National Taiwan University, Taipei, 106, Taiwan.
E-mail addresses: sychang@ntu.edu.tw (S.-Y. Chang), shihchung@ntu.edu.tw (S.-C. Chang).
[1] These authors contributed equally to this work.

https://doi.org/10.1016/j.antiviral.2022.105290
Received 9 December 2021; Received in revised form 19 February 2022; Accepted 12 March 2022
Available online 13 March 2022

SARS-CoV-2 neutralizing antibodies (NAbs), especially those derived from the COVID-19 convalescent patients' sera or B cells, have been reported with great potency to block RBD interaction with ACE2 and to inhibit SARS-CoV-2 infection *in vitro* (Cao et al., 2020; Chen et al., 2020; Hansen et al., 2020; Ju et al., 2020; Liu et al., 2020; Wan et al., 2020; Wang et al., 2020a; Wu et al., 2020; Zost et al., 2020). Some of the NAbs also exhibit prophylactic or therapeutic functionality against SARS-CoV-2 infection in animal experiments (Fedry et al., 2021; Liu et al., 2020; Wang et al., 2020c; Zost et al., 2020). Since RBD directly mediates virus engagement with ACE2, characterization of the epitopes in the RBD will provide valuable information for vaccine design, and are very helpful for the development of peptide drugs and small molecule inhibitors.

Although the epitopes of many potent NAbs have been shown to overlap with the ACE2 binding site on RBD, the arise of some SARS-CoV-2 variants has recently been reported with various types of immune escape mutations at the same region, leading to loss of the neutralizing activity of NAbs (Di Caro et al., 2021; Zhou et al., 2021a). Moreover, as SARS-CoV-2 continues to circulate globally, the viral variants that escape the selective pressure of NAbs may continue to emerge through the population-level immunity elicited by natural infection and vaccination. In addition, although a wide range of human antibodies is elicited by natural infection with SARS-CoV-2, only a small subset of induced antibodies exhibits high neutralizing potency (Zost et al., 2020). Therefore, more NAbs either directly neutralizing SARS-CoV-2 or facilitating the immune clearances of virus particles are still needed for being delivered therapeutically alone, or in combination with other NAbs to offer greater protection to immune-escaped SARS-CoV-2 variants. We now describe our efforts in isolating two mouse monoclonal antibodies (mAbs) 7 Eb-4G and 1Ba–3H by using the conventional hybridoma technology with the SARS-CoV-2 RBD as the immunogen. Both of 7 Eb-4G and 1Ba–3H target the RBM but only the later one shows neutralizing activity against SARS-CoV-2, indicating that the antigenic epitope in the RBM may not surely guarantee to induce potent NAbs. The site-directed mutagenesis assay was performed for identification of the antigenic determinants recognized by 1Ba–3H in the RBM, revealing that the binding epitope of 1Ba–3H is located in the region of residues 480–491. The plaque reduction assay was also applied for examination of the neutralizing activity of 1Ba–3H against the circulating SARS-CoV-2 Alpha, Epsilon, Gamma, and Delta variants of concern.

2. Materials and methods

2.1. Expression of the recombinant S, NTD and RBD proteins in human cells

The cDNA encoding for the amino acid sequence valine-16 to glutamine-1208 of SARS-CoV-2 S protein (GenBank accession no. **BCN86353.1**) with R682A, R683A, and R685A mutations, valine-16 to lysine-310 of SARS-CoV-2 S (for simplicity, hereafter referred to as NTD), or asparagine-331 to alanine-520 of SARS-CoV-2 S (for simplicity, hereafter referred to as RBD) was PCR-amplified from a mammalian codon-optimized S gene sequence (GenScript, Cat. No. MC_0101081), and then subcloned into the pSectag2A vector (Thermo Fisher Scientific) with an N-terminal secretion signal and a C-terminal hexa-histidine tag (His-tag). The recombinant proteins were expressed by using the Expi293 Expression System (Thermo Fisher Scientific) according to the manufacturer's instruction with minor modifications. Briefly, Expi293F cells (4×10^6 cell/mL) were cultured in Expi293F Expression medium (Thermo Fisher Scientific) in a 37 °C incubator with 80% humidity and 8% CO_2 on an orbital shaker shaking at 125 rpm, and transfected with the mixture of the previously described pSectag2A vector and the ExpiFectamine 293 Reagent (Thermo Fisher Scientific). Twenty hours post infection, the ExpiFectamine 293 Transfection Enhancers 1 and 2 were added to the medium and cultured for up to 7 days. Culture medium was collected by centrifugation at 4000×*g* for 30 min, and supernatant was filtered through a 0.22 μm bottle-top filter. The His-tagged protein was purified using the Ni-NTA resin (MAM-50 His_NTA resin, EBL Biotechnology) with the binding buffer (20 mM NaH_2PO_4, 0.5 M NaCl, 5 mM imidazole, pH 7.4) and the elution buffer (20 mM NaH_2PO_4, 0.5 M NaCl, 0.5 M imidazole, pH 7.4). Buffer exchange of the purified His-tagged protein solution with phosphate buffered saline (PBS) was performed by using the PD-10 desalting column (GE Healthcare). The protein concentration was determined by the Bradford dye-binding method (Bradford, 1976).

2.2. Expression of RBD truncation fragments in bacterial cells

The cDNA encoding for RBD, RBD-N (residues 331–436 of S), or the receptor binding motif (RBM; residues 437–506 of S) was subcloned into the pET30a vector (Novagen, Merck Group) with a C-terminal His-tag. The cDNA encoding for RBM1 (residues 437–456 of S), RBM2 (residues 457–476 of S), RBM3 (residues 477–496 of S), or RBM4 (residues 497–506 of S) was subcloned into the pET30a vector with an N-terminal superfolder GFP (sfGFP) (Pedelacq et al., 2006) and a C-terminal His-tag. The bacterial expression vectors were transformed into *Escherichia coli* (*E. coli*) BL21(DE3) competent cells and cultured in Luria-Bertani medium with kanamycin (50 μg/mL) at 37 °C on an orbital shaker. Protein expression was induced at an A_{600} of 0.4–0.6 by adding isopropyl-1-thio-beta-D-galactopyranoside to a final concentration of 1 mM for 4 h. Cells were collected by centrifugation at 8000×*g* for 10 min and the cell pellet was homogenized by cell disruptor (Constant Systems Limited, UK) in buffer A (20 mM sodium phosphate, 20 mM imidazole, 0.5 M NaCl, pH 7.4). The His-tagged protein was purified by using the HisTrap FF column (GE Healthcare) and the bound proteins were eluted with a 20–500 mM gradient of imidazole in buffer A. The purified His-tagged protein solution was then exchanged buffer with PBS by using the PD-10 desalting column (GE Healthcare). The protein concentration was determined by the Bradford dye-binding method.

2.3. Preparation of mouse mAbs against RBD

The animal experiment was approved by the Institutional Animal Care and Use Committee (IACUC) of National Taiwan University (Approval Number: NTU-109-EL-00051) and implemented in accordance with the animal care and ethics guidelines. The procedures for hybridomas production were performed as described previously (Cheng and Chang, 2021; Chiang et al., 2021) with slight modifications. In brief, two BALB/c male mice were immunized in a 2-week interval through intraperitoneal injection with a mixture of purified RBD (100 μg) and complete or incomplete Freund's adjuvant (0.25 mL) (Sigma-Aldrich), followed by a final booster injection of purified RBD (50 μg) in PBS. The myeloma Sp2/0-Ag14 cells (ATCC CRL-1581) were fused with splenocytes from donor mice at a 1:5 ratio of cell numbers in the presence of 0.7 mL polyethylene glycol 1500 (Sigma-Aldrich), and incubated at 37 °C for 2 min with gentle shaking. Additional 10 mL of Dulbecco's Modified Eagle Medium (DMEM) was then added to the cell mixture within 4 min. Cells were collected by centrifugation and resuspended in 30 mL of DMEM with 15% fetal bovine serum (FBS), 1% penicillin-streptomycin, 1 mM sodium pyruvate (Thermo Fisher Scientific), HybriMore Hybridoma Culture Supplement (Energenesis Biomedical, Taipei, Taiwan), and HAT media supplement (Sigma-Aldrich). Fusion cells were then cultured in the 96-well plates at 37 °C in the 5% CO_2 incubator. On days 3 and 7 post cell fusion, 100 μL of HT media supplement (Sigma-Aldrich) was added to the culture media. The culture media were collected on day 14 for performing the enzyme-linked immunosorbent assay (ELISA) by using the purified S as the antigen to screen for the positive hybridoma clones. The mAbs were further obtained by the limiting dilution method. To purify the mAbs, the hybridoma cell culture media were filtered through a 0.45 μm membrane disc and then purified by HiTrap Protein G HP column (GE Healthcare). The purified antibody was dissolved in PBS and the

concentration was determined by Bradford dye-binding method using mouse IgG as the standard.

2.4. ELISA

The wells of a 96-well plate pre-coated with 100 ng of S protein of SARS-CoV-2, SARS-CoV (Sino Biological Inc., Catalog Number: 40634-V08B), or MERS-CoV (Sino Biological Inc., Catalog Number: 40069-V08B) were blocked with 0.25% gelatin in PBS buffer containing 0.05% Tween-20 (PBST), and then incubated with 100 μL of indicated mAbs at room temperature for 1 h. After washing of the 96-well plate three times with PBST, the HRP-conjugated goat anti-mouse IgG (H + L) (KPL) was added to each well and incubated at room temperature for 1 h. After washing of the 96-well plate three times with PBST, 75 μL of 3,3′,5,5′-tetramethylbenzidine substrate (BD Bioscience) was added to each well for signal detection, followed by addition of 75 μL of 2 N H_2SO_4 to terminate the reactions. Results are evaluated quantitatively by measuring the absorbance at 450 nm by the Multiska FC Microplate Photometer (Thermo Fisher Scientific).

2.5. ACE2-transfected stable cell line

The human ACE2 mammalian expression vector pCMV3-C-His-ACE2 (GenBank accession no. **NM_021804.1**) was purchased from Sino Biological Inc. (Catalog Number: HG10108-CH), and then transfected to human embryonic kidney 293T (293T) cells by using the Lipofectamine 3000 reagent (Invitrogen, USA) according to the manufacturer's instruction. Twenty-four hours post transfection, 150 μg/mL of hygromycin (InvivoGen, USA) was added to the culture medium for selection of the ACE2-transfected 293T stable cell line (named as ACE2-293T). After obtaining the stable cell line, the collected cell samples were resuspended in lysis buffer (50 mM Tris-HCl, pH 7.4, 0.15 M NaCl, 0.25% deoxycholic acid, 1% NP-40, 1 mM EDTA) and subjected to SDS-PAGE and Western blotting (WB) analysis with anti-His tag antibody to confirm the expression of ACE2.

2.6. Pseudotyped virus neutralization assay

The SARS-CoV-2 S protein (wild type without D614G mutation) pseudotyped lentivirus containing with the enhanced GFP (EGFP) reporter gene or the luciferase reporter gene was obtained from the National RNAi Core Facility at Academia Sinica in Taiwan. One day before pseudoviral infection, 5×10^4 of ACE2-293T cells were seeded in the 96-well plate. On the day of pseudoviral infection, pseudotyped lentiviruses with a multiplicity of infection (MOI) of 3 were diluted in 200 μL of DMEM mixed with or without the serially diluted mAbs, and then incubated at 37 °C for 1 h. The mixtures were transferred to the ACE2-293T cell culture supplemented with DMEM and 10% FBS for 24 h at 37 °C in the 5% CO_2 incubator. After that, cells were washed and cultured with fresh medium for additional 48 h. The pseudotyped virus neutralization effect was determined by fluorescence microscopy or developed with One-Glo Luciferase Assay System (Promega) for reading the relative light unit (RLU) by a luminometer (Orion II; Berthod, Bad Wildbad, Germany). The titer of the neutralizing antibody was calculated as 50% inhibitory concentration (IC50) compared to the isotype control antibody. The IC50 of the neutralizing antibody was calculated using the Quest Graph IC50 Calculator (AAT Bioquest, Inc.).

2.7. In vitro RBD-ACE2 binding assay

The cDNA encoding for RBD was subcloned into the pTT5 vector with an N-terminal secretion signal and a C-terminal human Fc tag (referred to as RBD-hFc). The cDNA encoding for the ectodomain of human ACE2 was subcloned into the pSecTag2A vector with an N-terminal secretion signal and a C-terminal His tag. The recombinant RBD-hFc and ACE2 proteins were expressed as secreted proteins in the culture media by using the Expi293 Expression System with transfection of pTT5-SP-RBD-hFc and pSecTag2A-ACE2-His according to the manufacturer's instruction. The cell culture supernatants were collected for the subsequent purification procedures. RBD-hFc was purified by using the HiTrap Protein A HP column (GE Healthcare) and ACE2 was purified by using the HisTrap FF column (GE Healthcare) according to the manufacturer's instructions. The purified RBD-hFc and ACE2 were dialyzed with PBS. For conducting the *in vitro* RBD-ACE2 binding assay by competitive ELISA, 100 ng of purified ACE2 in 100 μL PBS was coated on the 96-well plate, which was subsequently blocked with 0.25% gelatin in PBST at 37 °C for 3 h. Additionally, 100 μL of purified RBD-hFc (2.5 μg/mL) in PBS was pre-incubated with various amounts of 1Ba–3H (1–20 μg/mL) at 37 °C for 1 h and then added to the 96-well plate, which was pre-coated with ACE2. After washing the plate three times with PBST, the HRP-conjugated goat anti-human IgG secondary antibody (Bethyl Laboratories, CAT # A80-119) was added to detect the RBD-hFc which remained binding to ACE2. The signal detection were performed as described in ELISA method. Results are evaluated quantitatively by measuring the absorbance at 450 nm by the Multiska FC Microplate Photometer (Thermo Fisher Scientific). Inhibition of RBD-ACE2 binding by 1Ba–3H was calculated according to the absorbance in the presence of various amounts of 1Ba–3H as compared with that detected in the absence of 1Ba–3H.

2.8. Site-directed mutagenesis

The cDNA encoding for RBD was subcloned into the pET30a vector (Novagen, Merck Group) with a C-terminal His-tag and an N-terminal superfolder GFP (sfGFP) fusion tag to increase the protein solubility (Pedelacq et al., 2006). The pET30a-sfGFP-RBD-His plasmid was used as the template for site-directed mutagenesis. The codons encoding for the amino acid residues 477–495 in the RBD were substituted individually with the codons of alanine by using the PCR-based site-directed mutagenesis method. All mutations were confirmed by Sanger sequencing. The vectors for expressing the sfGFP-RBD-His mutants were transformed into *E. coli* BL21(DE3) competent cells, and the protein expression were induced as described previously. Bacterial cells were collected for protein extraction, which was then subjected to SDS-PAGE and WB analysis with the anti-His tag antibody and 1Ba–3H.

2.9. Plaque reduction assay

All experiments related to plaque reduction assay were performed in the biosafety-level 3 (BSL-3) laboratory. Antibody solution was incubated with 150 plaque forming units (PFU) of SARS-CoV-2 wild type strain (EPI_ISL_422415; A.3), Alpha (EPI_ISL_1010728; B.1.1.7), Gamma (EPI_ISL_2249499; P.1), Delta (EPI_ISL_3979387; B.1.617.2), or Epsilon (EPI_ISL_1020315; B.1.429) variant in the presence of DMEM containing with 8 μg/mL TPCK-trypsin for 1 h at 37 °C. Antibody-virus mixtures (200 μL/well) were subsequently added to the Vero E6 cell monolayers cultured in the 24-well plates. After 1 h, cells were washed with PBS, overlaid with 2% (w/v) methylcellulose in DMEM supplemented with 2% FBS, and then incubated at 37 °C in the 5% CO_2 incubator. Five days later, cells were fixed with 10% formaldehyde in PBS for 1 h and stained with 0.5% crystal violet. After that, plaque numbers were counted and compared with the numbers obtained from the PBS control experiments to calculate the inhibition level.

2.10. Quantitative reverse transcription PCR (RT-qPCR)

To determine the expression level of the envelope (E) gene of SARS-CoV-2 by RT-qPCR, the Gamma variant at 0.002 or 0.01 MOI was pretreated with 100 μg/mL of 1Ba–3H for 1 h at 37 °C, respectively. The virus-antibody mixture was added to the Vero E6 cell monolayer for another 1 h at 37 °C. After incubation, virus was removed and washed once with PBS before adding DMEM with 2% FBS for 24 h. Total RNA

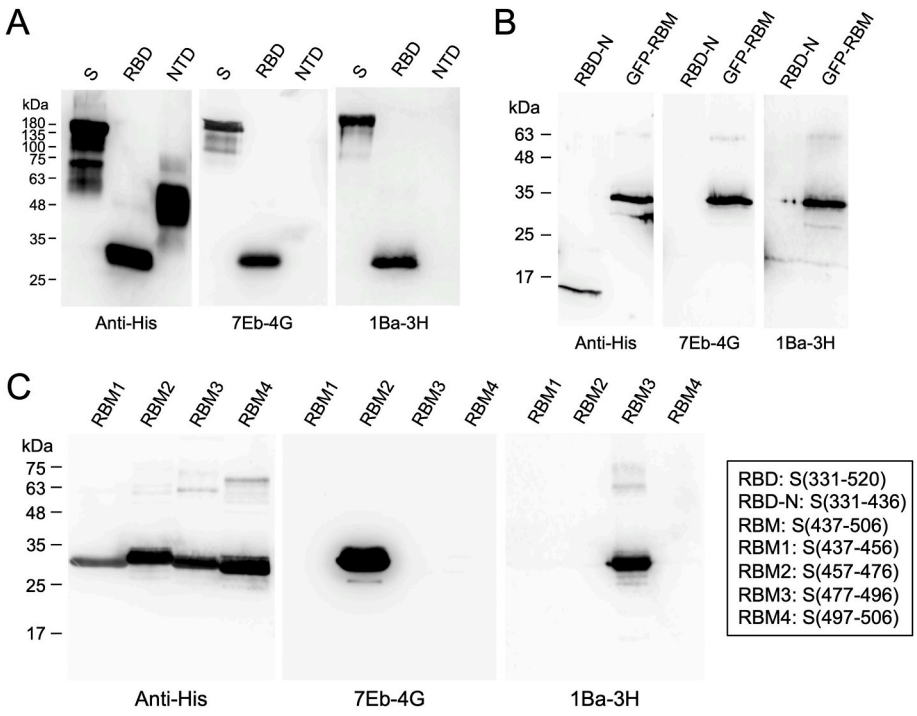

Fig. 1. Characterization of the binding specificity of 7 Eb-4G and 1Ba–3H by epitope mapping.
(A) The recombinant His-tagged S, RBD, and NTD proteins, (B) RBD-N and sfGFP-RBM, or (C) RBM1, RBM2, RBM3, and RBM4 were subjected to SDS-PAGE and WB analysis with anti-His tag antibody, 7 Eb-4G, and 1Ba–3H. Molecular weight standards in kDa unit were marked with small ticks. The sfGFP-RBM and sfGFP-RBM1-4 were abbreviated as GFP-RBM and RBM1-4 in figure. S, S(16–1208). RBD, S (331–520). NTD, S(16–310). RBD-N, S(331–436). RBM, S(437–506). RBM1, S(437–456). RBM2, S (457–476). RBM3, S(477–496). RBM4, S(497–506).

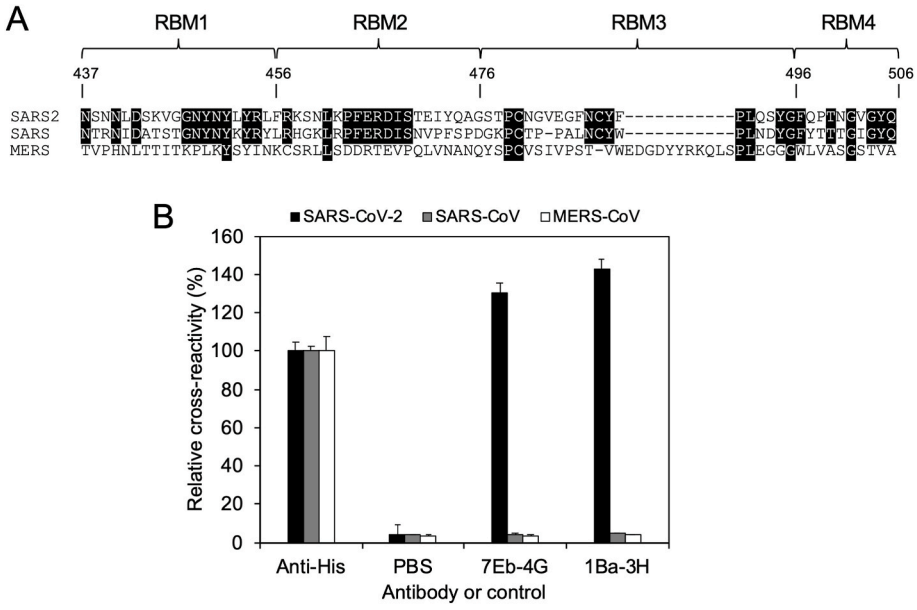

Fig. 2. Analysis of the cross-reactivity of 7 Eb-4G and 1Ba–3H with the S proteins derived from SARS-CoV-2, SARS-CoV, and MERS-CoV.
(A) Alignment of the amino acid sequences of RBMs derived from SARS-CoV-2 (GenBank accession no. **BCN86353.1**), SARS-CoV (GenBank accession no. **AAR86775.1**), and MERS-CoV (GenBank accession no. **AHE78097.1**). The identical residues among these three viruses or between SARS-CoV-2 and SARS-CoV were noted with black backgrounds. (B) The His-tagged S proteins of SARS-CoV-2 (black bars), SARS-CoV (gray bars), and MERS-CoV (white bars) were utilized as the antigens in the ELISA for analyzing the cross-reactivity of 7 Eb-4G and 1Ba–3H. The results showed that 7 Eb-4G and 1Ba–3H are highly specific to SARS-CoV-2 S protein.

was extracted from infected cells and then subjected to RT-qPCR assay by using the iTaq Universal Probes One-Step Kit (Bio-Rad, USA) and the QuantStudio 5 Real-Time PCR System (Thermo Fisher Scientific, USA) with the E-specific forward primer (5′-ACAGGTACGTTAATAGTTAATAGCGT-3′), reverse primer (5′-ATATTGCAGCAGTACGCACACA-3′), and probe (5′-FAM-ACACTAGCCATCCTTACTGCGCTTCG-BBQ-3′). Plasmid containing partial E gene sequence was used as the control.

3. Results

3.1. The SARS-CoV-2 RBD-specific mAbs 7 Eb-4G and 1Ba–3H

In order to generate the specific mAb for recognition of the RBD on the SARS-CoV-2 S protein, the recombinant RBD expressed in Expi293F cells was utilized as the immunogen for mouse immunization. By using the conventional cell-fusion hybridoma technology, two mAbs 7 Eb-4G and 1Ba–3H were selected for further biochemical characterization. 7 Eb-4G and 1Ba–3H showed great specificity for binding to S protein and RBD without having cross-reactivity with NTD (Fig. 1A). In addition, both of 7 Eb-4G and 1Ba–3H recognized the RBM, instead of RBD-N (Fig. 1B). Thereafter, the smaller RBM fragments (RBM1-4) fused with a C-terminal sfGFP tag were applied in the WB analysis to further identify the binding epitopes of 7 Eb-4G and 1Ba–3H. The results showed that the binding epitope of 7 Eb-4G is mainly located in the RBM2 within the region of S (457–476), and the binding epitope of 1Ba–3H is mainly located in the RBM3 within the region of S (477–496)

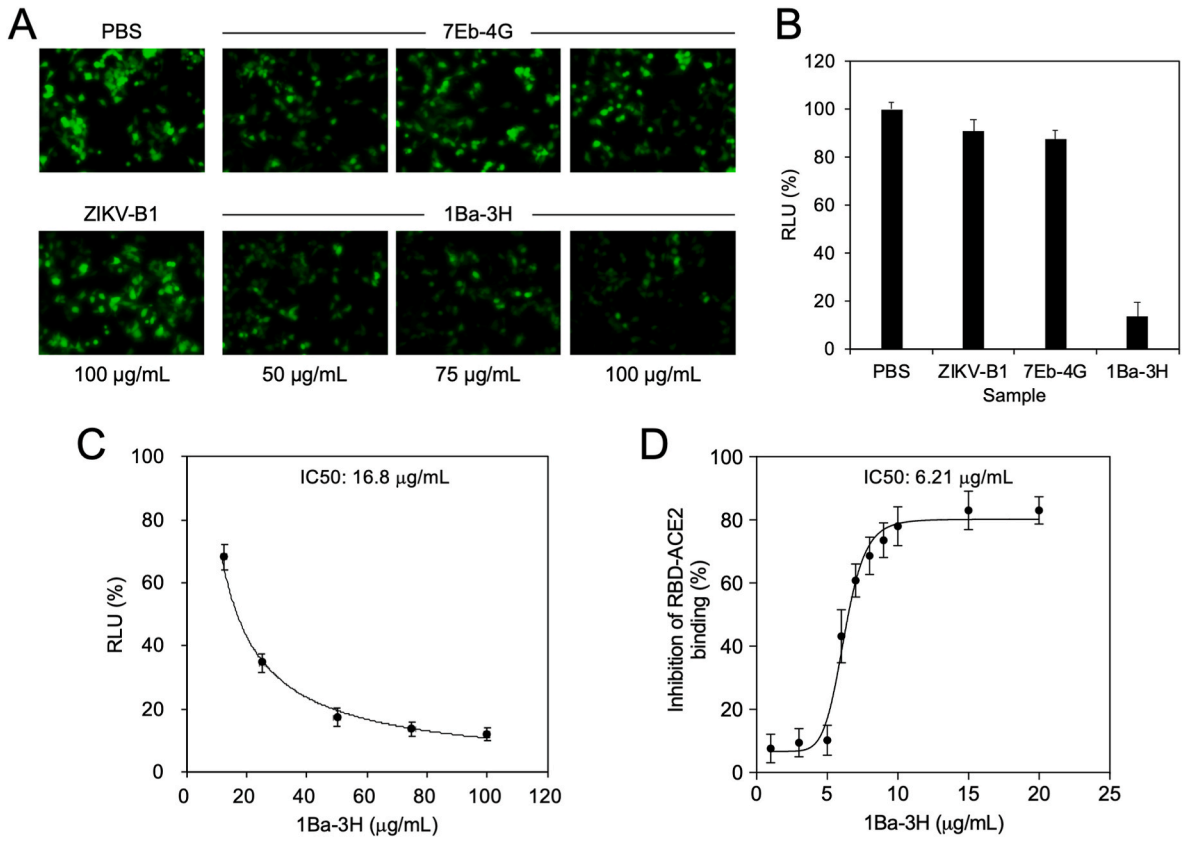

Fig. 3. Analysis of the neutralizing activity of 7 Eb-4G and 1Ba–3H using the pseudotyped virus infection assay and *in vitro* RBD-ACE2 binding assay.
(A) The pseudotyped lentivirus containing with the cell-surface expressed SARS-CoV-2 S protein and the internal EGFP reporter gene was incubated with PBS, ZIKV-B1 (100 μg/mL), 7 Eb-4G (50, 75, or 100 μg/mL), or 1Ba–3H (50, 75, or 100 μg/mL) at 37 °C for 1 h. The mixtures of pseudotyped lentiviruses and antibodies were transferred to ACE2-293T cells in the 96-well plate for 24 h at 37 °C in the 5% CO_2 incubator. After that, cells were washed and supplemented with fresh culture medium for additional 48 h of incubation. The pseudotyped virus neutralization effect was analyzed by fluorescence microscopy to reveal the EGFP expression level. The reduced EGFP expression level indicates the reduced infection by the pseudotyped lentivirus. Scale bar, 100 μm. (B) EGFP was replaced with luciferase as the reporter gene in the pseudotyped virus infection assay as described previously. The luciferase activity was developed with One-Glo Luciferase Assay System, and the relative light unit (RLU) was read on a luminometer. PBS, ZIKV-B1 (100 μg/mL), and 7 Eb-4G (100 μg/mL) did not have the neutralizing activity. In contrast, 1Ba–3H (100 μg/mL) can efficiently inhibit pseudotyped virus infection. (C) Different amounts of 1Ba–3H (12.5, 25, 50, 75, and 100 μg/mL) were applied in the pseudotyped virus infection assay to measure the RLU and calculate the IC50 values using the Quest Graph IC50 Calculator. (D) For conducting the *in vitro* RBD-ACE2 binding assay by competitive ELISA, 100 μL of RBD-hFc (2.5 μg/mL) in PBS was pre-incubated with various amounts of 1Ba–3H (1–20 μg/mL) at 37 °C for 1 h and then added to the 96-well plate, which was pre-coated with ACE2. After washing the plate three times with PBST, the HRP-conjugated goat anti-human IgG secondary antibody was added to detect the RBD-hFc which remained binding to ACE2. Inhibition of RBD-ACE2 binding was calculated according to the decreased detection signal in the presence of 1Ba–3H by comparing to the result of PBS control. Data are presented as means ± SD of three independent experiments, and further graphed by the GraphPad Prism software.

(Fig. 1C).

Among the human coronaviruses, SARS-CoV and MERS-CoV are the most related viral strains with SARS-CoV-2 (Abdelrahman et al., 2020). Therefore, the amino acid sequences of the RBMs derived from SARS-CoV-2, SARS-CoV, and MERS-CoV are aligned to reveal their identity and similarity (Fig. 2A). It is noted that the amino acid sequences of MERS-CoV RBM are different from those of SARS-CoV-2 and SARS-CoV. Especially, there is an extra insertion in the MERS-CoV RBM3 (Fig. 2A). Although certain residues in RBMs of SARS-CoV-2 and SARS-CoV are identical, a large portion of RBM2 and RBM3 are quite dissimilar between these two viruses. To further clarify the specificity of 7 Eb-4G and 1Ba–3H, the recombinant S proteins of SARS-CoV-2, SARS-CoV and MERS-CoV were utilized to perform the ELISA. The results showed that 7 Eb-4G and 1Ba–3H are highly specific to the SARS-CoV-2 S protein without exhibiting cross-reactivity with the S proteins of SARS-CoV and MERS-CoV (Fig. 2B).

3.2. 1Ba–3H inhibits pseudotyped virus infection

Since RBM is the critical part of SARS-CoV-2 S protein for mediating virus binding to ACE2, it has been demonstrated that antibody targeting to RBM might have neutralizing functionality. The pseudotyped lentivirus containing with the cell-surface expressed SARS-CoV-2 S protein and the internal EGFP or luciferase reporter gene was utilized to examine whether 7 Eb-4G and 1Ba–3H can inhibit the pseudotyped virus infection in ACE2-293T cells. The results showed that the isotype control antibody ZIKV-B1(Li et al., 2021) and 7 Eb-4G did not have any neutralizing activity since the EGFP was successfully expressed upon pseudotyped virus infection in ACE2-293T cells (Fig. 3A). In contrast, 1Ba–3H performed strong neutralizing activity as the expression of EGFP in ACE2-293T cells was markedly inhibited (Fig. 3A). In another attempt using the luciferase gene as the reporter cassette in the neutralization assay, the experimental results also showed that only 1Ba–3H can efficiently block pseudotyped virus infection in ACE2-293T cells (Fig. 3B). To further determine the IC50 of 1Ba–3H, the serially diluted 1Ba–3H (12.5–100 μg/mL) were applied in the pseudotyped virus neutralization assay. As the concentration of the 1Ba–3H increased, the luciferase expression levels were markedly reduced (Fig. 3C). The IC50 value of 1Ba–3H for neutralizing pseudotyped virus infection in ACE2-293T cells is about 16.8 μg/mL. Next, the *in vitro*

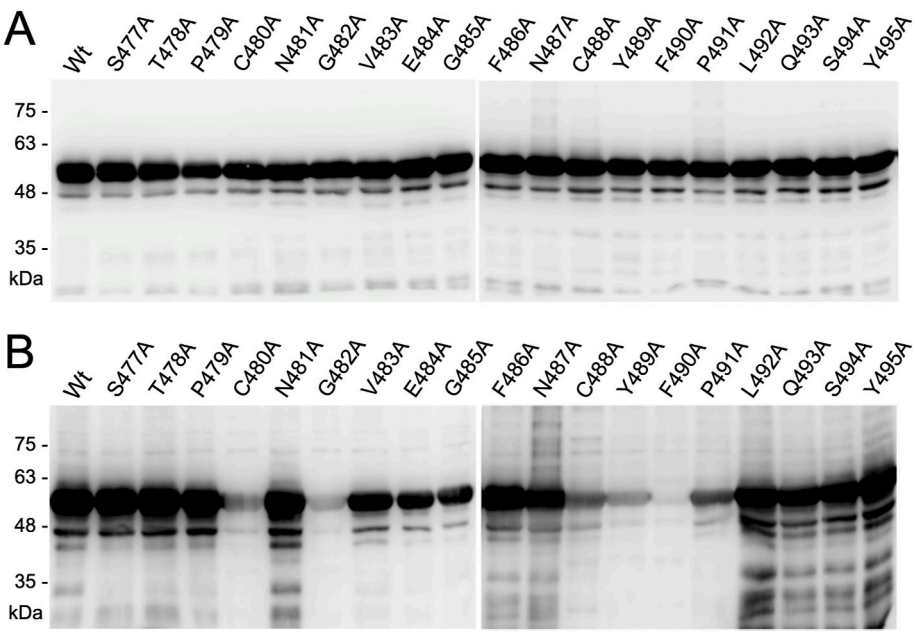

Fig. 4. Analysis of the binding epitope of 1Ba-3H
The recombinant sfGFP-RBD-His mutants with a series of individual alanine substitutions at residues 477–495 were expressed in *E. coli* and the bacterial cell lysates (10 μg) were subjected to SDS-PAGE and WB analysis with anti-His tag antibody (A) and 1Ba–3H (B) to identify the critical antigenic determinants. The loss of WB signal in a specific mutation represents the indicated residue is required for interaction with 1Ba–3H.

RBD-ACE2 competitive binding assay was applied to examine whether 1Ba–3H can block the binding between RBD and ACE2. RBD-hFc was pre-incubated with various amounts of 1Ba–3H (1–20 μg/mL) and then added to the 96-well plate, which was pre-coated with ACE2. The RBD-hFc which remained binding to ACE2 in the presence of 1Ba–3H was detected by the HRP-conjugated goat anti-human IgG secondary antibody. The results of the competitive ELISA showed that the binding between RBD and ACE2 was gradually inhibited by pre-incubation of RBD-hFc with the increasing amounts of 1Ba–3H (Fig. 3D). The IC50 value of 1Ba–3H obtained in the competitive ELISA is about 6.21 μg/mL (Fig. 3D).

3.3. Identification of the antigenic determinants in the RBD recognized by 1Ba–3H

Several SARS-CoV-2 variants with L452R, E484K, and N501Y mutations in the S protein have recently drawn a lot of public health attentions since these variants exhibit better spreading capability or greater resistance to NAb (Davies et al., 2021; Di Caro et al., 2021; Zhou et al., 2021a). As demonstrated previously, the binding epitope of 1Ba–3H is mainly located within the region of S (477–496) (Fig. 1C). To identify the critical antigenic determinants recognized by 1Ba–3H, the amino acid residues 477–495 in the RBD were substituted with alanine individually to generate a series of RBD mutants for WB analysis with the control anti-His tag antibody (Fig. 4A), and 1Ba–3H (Fig. 4B). The results clearly showed that residues 480, 482, 484, 485, and 488–491 in the RBD are the critical antigenic determinants for 1Ba–3H recognition, since replacement of these residues with an alanine abrogated or inhibit the binding of 1Ba–3H (Fig. 4B). Notably, 1Ba–3H exhibited a reduced capability for binding to RBD with an E484A mutation, implying that 1Ba–3H might lose its neutralizing activity against SARS-CoV-2 variants with a sequence mutation at E484 of S protein.

3.4. Neutralization or enhanced infection of SARS-CoV-2 variants by 1Ba–3H

To further investigate whether 1Ba–3H can neutralize diverse SARS-CoV-2 variants, the plaque reduction assay was performed to analyze the neutralizing activity of 1Ba–3H against SARS-CoV-2 wild type, Alpha (with an N501Y mutation), Gamma (with K417T, E484K and N501Y mutations), Delta (with L452R and T478K mutations), and Epsilon (with an L452R mutation) variants. As shown in Fig. 5A, 1Ba–3H exhibited neutralizing activity against Alpha, Epsilon, and Delta variants, but lost neutralizing activity against Gamma variant. It is noted that Gamma variant contains with an E484K mutation in the S protein, which may lead to blockage of 1Ba–3H binding. The data also showed that 1Ba–3H exhibited stronger neutralizing activity against Alpha, Epsilon, and Delta variants than the wild type strain (Fig. 5B). Surprisingly, we found that 1Ba–3H can enhance the cellular infection of Gamma variant (Fig. 5B). The results suggest that 1Ba–3H may lose its neutralizing activity against the SARS-CoV-2 variant with an E484K mutation in the S protein and adversely cause antibody-dependent enhancement (ADE) of virus infection. To investigate whether the ADE of infection was a dose-dependent response mediated by 1Ba–3H, SARS-CoV-2 Gamma variant virus (MOI: 0.0005) was pre-incubated with the various amounts of 1Ba–3H (0, 25, 50, and 100 μg/mL), and then added to the Vero E6 cell monolayers for performing the plaque reduction assay. The results showed that the numbers of plaques increased dose-dependently with the amounts of 1Ba–3H utilized in the experiments (Fig. 5C). Additionally, the virus yield reduction assay was performed by pre-incubation of various amounts of Gamma variant virus (MOI: 0.002 and 0.01) with the same amount of 1Ba–3H (100 μg/mL), before adding to Vero E6 cell monolayers for 24 h. The titer of infectious virus in the culture supernatant was quantified by plaque assay. However, there is no statistical difference in the plaque numbers between the presence and absence of 1Ba–3H (Fig. 5D), indicating that the virus infection efficiency was not further enhanced in the presence of 1Ba–3H while a 4-fold or 10-fold higher virus input was utilized in the yield reduction assay. The RT-qPCR was also applied for analyzing the expression level of SARS-CoV-2 E gene. The results showed that a slightly increased expression of E gene was observed in the presence of 1Ba–3H than the PBS control under the experimental condition using 0.002 MOI of Gamma variant virus (Fig. 5E). In contrast, there is no significant difference in the E gene expression level between the presence and absence of 1Ba–3H while using 0.01 MOI of Gamma variant virus in the experiment (Fig. 5E). The capability of 1Ba–3H to enhance Gamma variant infection was observed at lower virus input in the plaque reduction assay, while such phenomenon was not observed when a high viral titer was employed in the virus yield reduction assay.

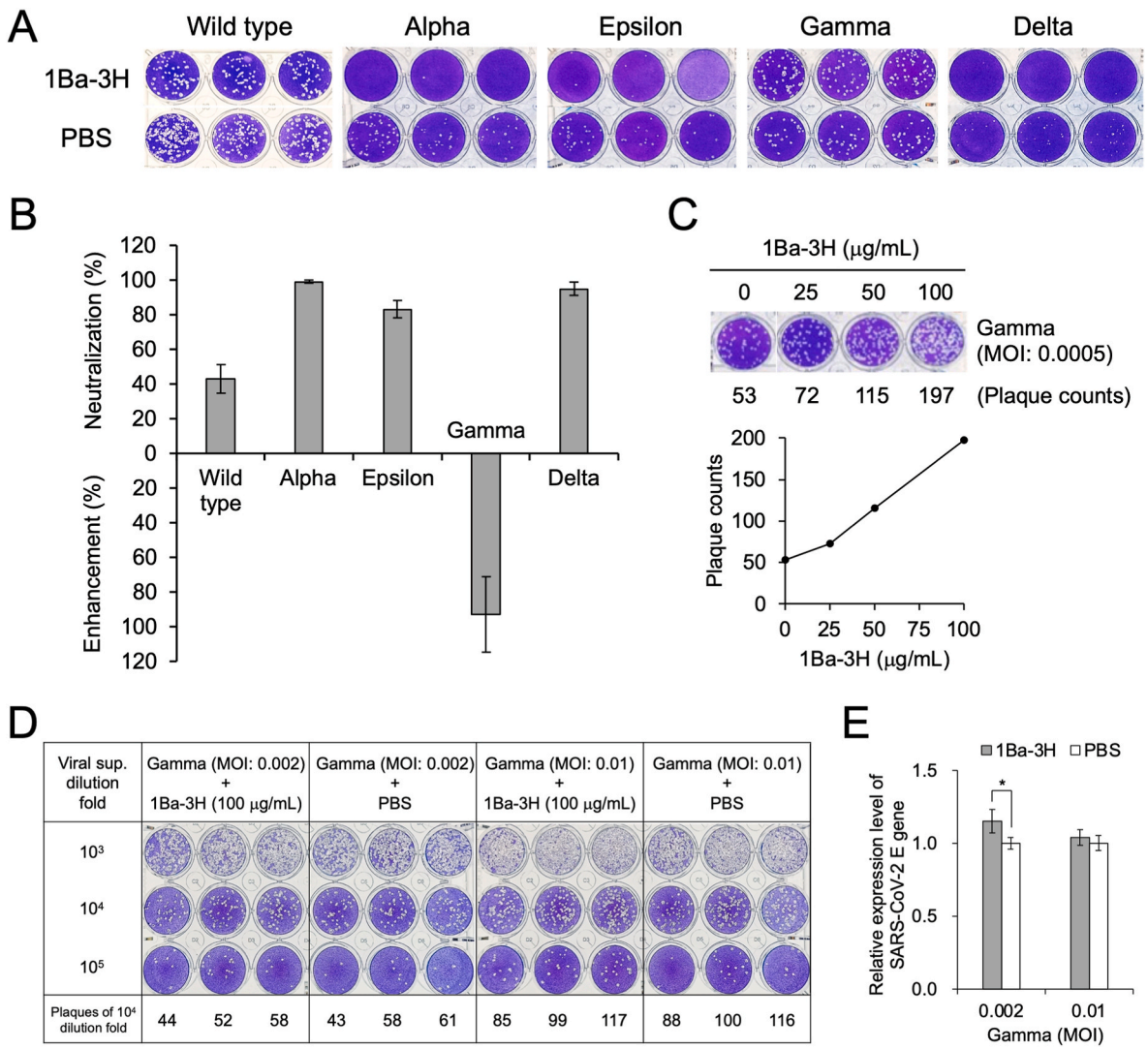

Fig. 5. 1Ba–3H can neutralize diverse SARS-CoV-2 variants. (A) For performing the plaque reduction assay, 1Ba–3H (200 μg/mL) was pre-incubated with 150 PFU of the SARS-CoV-2 wild type, Alpha, Gamma, Delta, and Epsilon variants for 1 h at 37 °C. Antibody-virus mixtures were subsequently added to Vero E6 cell monolayers in the 24-well plates. After 1 h, cells were washed and overlaid with methylcellulose in the culture medium. Five to seven days later, plates were fixed with formaldehyde and stained with crystal violet. (B) Plaques were counted. The inhibition of the plaque formation by 1Ba–3H was calculated by comparing to the result derived from the experiments using PBS. Data are presented as means ± SD of three independent experiments. (C) The various amounts of 1Ba–3H (0–100 μg/mL) were pre-incubated with SARS-CoV-2 Gamma variant (MOI: 0.0005) for 1 h at 37 °C. Antibody-virus mixtures were subsequently added to Vero E6 cell monolayers in the 24-well plates for performing the plaque reduction assay. Plaque counts were provided below the wells stained with crystal violet and further plotted with the amounts of 1Ba–3H as shown in the line graph. (D) The various amounts of SARS-CoV-2 Gamma variant (MOI: 0.002 and 0.01) were pre-incubated with 1Ba–3H (100 μg/mL) for 1 h at 37 °C. Antibody-virus mixtures were subsequently added to Vero E6 cell monolayers in the 24-well plates. After 24 h, the viral culture supernatants were collected, diluted 10^3–10^5 folds, and then added to Vero E6 cell monolayers in the 24-well plates for performing the plaque assay to quantify the titer of infectious virus. Plaque counts of the experimental groups of 10^4 dilution fold were provided. (E) For analyzing the expression level of the SARS-CoV-2 E gene, the viral culture supernatants described above were subjected to RT-qPCR by using the E-specific forward, reverse, and probe oligos. Data are presented as means ± SD of three independent experiments. The statistical significance was calculated with Student's t-test. * represents $P \leq 0.05$.

4. Discussion

It has been demonstrated that the RBD-specific antibody may not always have the capability to neutralize SARS-CoV-2 infection (Brouwer et al., 2020). Indeed, the present study showed that 7 Eb-4G does not have the neutralizing activity even though it can bind to the RBM2 region in the RBD. This result implies that using RBD as the immunogen for vaccination may not necessarily guarantee for induction of antibodies with the neutralizing activity. In contrast, 1Ba–3H, an RBM3-specific mAb, can efficiently prevent SARS-CoV-2 infection in Vero E6 cells. The three-dimensional structure of the RBD and ACE2 complex has already been reported (Hoffmann et al., 2020; Lan et al., 2020; Shang et al., 2020; Wang et al., 2020b; Yan et al., 2020). In order to localize the binding epitopes of 7 Eb-4G and 1Ba–3H, the regions of RBM1-4 are labelled individually with different colors in the RBD and ACE2 complex (Wang et al., 2020b) (Fig. 6A). The images show that the large majority of RBD-N (gray color in Fig. 6A) and RBM2 (cyan color in Fig. 6A) are away from the RBD and ACE2 binding interface, except there is a direct interaction of K417 with ACE2. Since the binding epitope of 7 Eb-4G is located in the RBM2, it's not surprising that 7 Eb-4G couldn't inhibit RBD binding to ACE2 (Fig. 3). On the contrary, the large parts of RBM1 (yellow color in Fig. 6A), RBM3 (red color in Fig. 6A), and RBM4 (magenta color in Fig. 6A) are located in the RBD and ACE2 binding interface. Previous studies have shown that several key residues in RBD-N (K417), RBM1 (G446, Y449, Y453, L455, and F456), RBM2 (Y473, A475, and G476), RBM3 (E484, F486, N487, Y489,

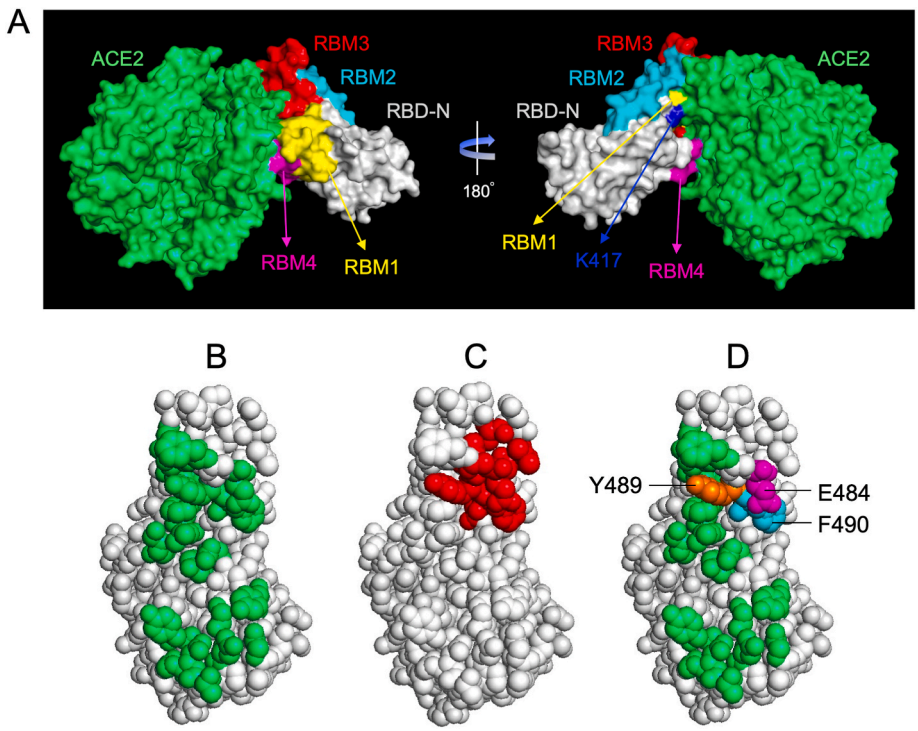

Fig. 6. Mapping of the binding epitope of 1Ba–3H on the three-dimensional structure of RBD and ACE2 complex. (A) The RBD and ACE2 complex (PDB code: 6lzg) was illustrated as the surface mode by using the PyMOL software. ACE2, green color. RBD-N, gray color. RBM1, yellow color. RBM2, cyan color. RBM3, red color. RBM4, magenta color. K417, blue color. The large majority of RBD-N and RBM2 are away from the RBD and ACE2 binding interface. Many key residues of RBM1, RBM3, and RBM4 are directly involved in interacting with ACE2, including the K417 in the RBD-N. (B) The key residues of the RBD which were involved in the direct interaction with ACE2 were marked in green color. (C) The antigenic determinants in the RBD (white color) recognized by 1Ba–3H were marked in red color. (D) Replacement of E484 (magenta), Y489 (orange), or F490 (cyan) with an alanine residue interrupted 1Ba–3H binding to RBD.

F490, Q493, and G496), and RBM4 (Q498, T500, N501, G502, and Y505) are directly involved in interaction with ACE2 (Kim et al., 2021; Yi et al., 2020) (Fig. 6B, residues in green color). Obviously, RBM3 is the most essential clutch for SARS-CoV-2 binding to ACE2 receptor. This study demonstrated that the antigenic determinants (residues 480, 482, 484, 485, and 488–491) in the RBD recognized by 1Ba–3H are located in the RBM3 (Fig. 6C, residues in red color). Therefore, we hypothesized that 1Ba–3H may block SARS-CoV-2 infection through preventing RBD binding to ACE2. By using the *in vitro* RBD-ACE2 binding assay, we found that 1Ba–3H can efficiently prevent RBD from binding to ACE2 in a dose-dependent manner (Fig. 3D). We also found that the neutralizing potency of 1Ba–3H is very low (IC50 = 16.8 or 6.21 μg/mL) compared to current therapeutic antibodies with IC50 values of <0.1 μg/mL. One of the possible reasons is that 1Ba–3H might be less resistant to trypsin treatment, which was applied in the plaque reduction assay, leading to the observation of the weaker neutralizing activity. Therefore, improvement of the stability of 1Ba–3H remains a challenge for the future development of therapeutics.

The ongoing global spread of SARS-CoV-2 led to the emergence of a large number of variants with higher transmissibility (Davies et al., 2021; Singh et al., 2021). The immune escape variants frequently carry sequence mutations at the ACE2-interacting residues in the RBD (Gomez et al., 2021; Harvey et al., 2021), that makes the discovery of potent neutralizing antibodies more challenging. Some human NAbs that target the RBD of the SARS-CoV-2 S protein showed therapeutic promise and are being evaluated clinically (Hurt and Wheatley, 2021; Min and Sun, 2021). Here we found that 1Ba–3H exhibited great neutralizing activity against Alpha, Delta, and Epsilon variants (Fig. 6). On the contrary, 1Ba–3H lost its functionality against the Gamma variant, which contains with an E484K mutation in the S protein, and adversely enhanced virus infection. The ADE mediated by 1Ba–3H for infection of Vero E6 cells with lower viral titer of Gamma variant was observed in a dose-dependent manner (Fig. 5C). However, the capability of 1Ba–3H for neutralization or enhancement of Gamma variant infection was not observed when high viral titer was employed in the virus yield reduction assay (Fig. 5D and E), indicating that the virus infection efficiency was not further enhanced in the presence of 1Ba–3H while the viral titer was high.

Although the molecular basis for the ADE mediated by 1Ba–3H remained unknown, our findings clearly demonstrated that the "ADE of viral entry'' may happen when the binding epitope of 1Ba–3H was mutated in the virus variant. It has been reported that some RBD-specific antibodies could mediate ADE of SARS-CoV-2 entry in Raji cells via an Fcγ receptor-dependent mechanism (Zhou et al., 2021b). Therefore, for evaluation of the functionality of a SARS-CoV-2 NAb, it is essential to determine its binding epitopes in the S protein in order to have better understanding about the potential neutralizing activity or the possible ADE of viral entry.

Authors' contributions

G.-C.L., T.-L.C., S.-Y.L., S.-Y.C., and S.-C.C. conceived and designed research. S.-Y.C. and S.-C.C. acquired funds and conducted experiments. G.-C.L., T.-L.C., S.-Y.L., H.-C.K., and Y.-M.T. performed experiments. D.-C.L., and Y.-W.C. provided critical reagents and methods. G.-C.L., T.-L.C., S.-Y.L., S.-Y.C., and S.-C.C. analyzed data and wrote the manuscript.

Declaration of competing interest

The authors declare that they have no known competing financial interests or personal relationships that could have appeared to influence the work reported in this paper.

Acknowledgments

The authors are thankful to the excellent technical assistance from Center of Biotechnology, and Technology Commons, College of Life Science, National Taiwan University, and the National RNAi Core Facility at Academia Sinica in Taiwan for providing reagents and related services. We would also like to acknowledge the service provided by the Biosafety Level-3 Laboratory of the First Core Laboratory, National Taiwan University College of Medicine. This work was supported by the Ministry of Science and Technology, Taiwan [grant numbers MOST-110-2311-B-002-010 and MOST109-2327-B-002-009] and National Taiwan

University [grant numbers 109L883703 and 110L880802].

References

Abdelrahman, Z., Li, M., Wang, X., 2020. Comparative review of SARS-CoV-2, SARS-CoV, MERS-CoV, and influenza A respiratory viruses. Front. Immunol. 11, 552909.

Bradford, M.M., 1976. A rapid and sensitive method for the quantitation of microgram quantities of protein utilizing the principle of protein-dye binding. Anal. Biochem. 72, 248–254.

Brouwer, P.J.M., Caniels, T.G., van der Straten, K., Snitselaar, J.L., Aldon, Y., Bangaru, S., Torres, J.L., Okba, N.M.A., Claireaux, M., Kerster, G., Bentlage, A.E.H., van Haaren, M.M., Guerra, D., Burger, J.A., Schermer, E.E., Verheul, K.D., van der Velde, N., van der Kooi, A., van Schooten, J., van Breemen, M.J., Bijl, T.P.L., Sliepen, K., Aartse, A., Derking, R., Bontjer, I., Kootstra, N.A., Wiersinga, W.J., Vidarsson, G., Haagmans, B.L., Ward, A.B., de Bree, G.J., Sanders, R.W., van Gils, M. J., 2020. Potent neutralizing antibodies from COVID-19 patients define multiple targets of vulnerability. Science 369, 643–650.

Cao, Y., Su, B., Guo, X., Sun, W., Deng, Y., Bao, L., Zhu, Q., Zhang, X., Zheng, Y., Geng, C., Chai, X., He, R., Li, X., Lv, Q., Zhu, H., Deng, W., Xu, Y., Wang, Y., Qiao, L., Tan, Y., Song, L., Wang, G., Du, X., Gao, N., Liu, J., Xiao, J., Su, X.D., Du, Z., Feng, Y., Qin, C., Qin, C., Jin, R., Xie, X.S., 2020. Potent neutralizing antibodies against SARS-CoV-2 identified by high-throughput single-cell sequencing of convalescent patients' B cells. Cell 182, 73–84.

Chen, X., Li, R., Pan, Z., Qian, C., Yang, Y., You, R., Zhao, J., Liu, P., Gao, L., Li, Z., Huang, Q., Xu, L., Tang, J., Tian, Q., Yao, W., Hu, L., Yan, X., Zhou, X., Wu, Y., Deng, K., Zhang, Z., Qian, Z., Chen, Y., Ye, L., 2020. Human monoclonal antibodies block the binding of SARS-CoV-2 spike protein to angiotensin converting enzyme 2 receptor. Cell. Mol. Immunol. 17, 647–649.

Cheng, Y.C., Chang, S.C., 2021. Development and biochemical characterization of the monoclonal antibodies for specific detection of the emerging H5N8 and H5Nx avian influenza virus hemagglutinins. Appl. Microbiol. Biotechnol. 105, 235–245.

Chiang, Y.W., Li, C.J., Su, H.Y., Hsieh, K.T., Weng, C.W., Chen, H.W., Chang, S.C., 2021. Development of mouse monoclonal antibody for detecting hemagglutinin of avian influenza A(H7N9) virus and preventing virus infection. Appl. Microbiol. Biotechnol. 105, 3235–3248.

Davies, N.G., Abbott, S., Barnard, R.C., Jarvis, C.I., Kucharski, A.J., Munday, J.D., Pearson, C.A.B., Russell, T.W., Tully, D.C., Washburne, A.D., Wenseleers, T., Gimma, A., Waites, W., Wong, K.L.M., van Zandvoort, K., Silverman, J.D., Group, C. C.-W., Consortium, C.-G.U., Diaz-Ordaz, K., Keogh, R., Eggo, R.M., Funk, S., Jit, M., Atkins, K.E., Edmunds, W.J., 2021. Estimated transmissibility and impact of SARS-CoV-2 lineage B.1.1.7 in England. Science 372 eabg3055.

Di Caro, A., Cunha, F., Petrosillo, N., Beeching, N.J., Ergonul, O., Petersen, E., Koopmans, M.P.G., 2021. Severe acute respiratory syndrome coronavirus 2 escape mutants and protective immunity from natural infections or immunizations. Clin. Microbiol. Infect. 27, 823–826.

Fedry, J., Hurdiss, D.L., Wang, C., Li, W., Obal, G., Drulyte, I., Du, W., Howes, S.C., van Kuppeveld, F.J.M., Forster, F., Bosch, B.J., 2021. Structural insights into the cross-neutralization of SARS-CoV and SARS-CoV-2 by the human monoclonal antibody 47D11. Sci. Adv. 7, eabf5632.

Gomez, C.E., Perdiguero, B., Esteban, M., 2021. Emerging SARS-CoV-2 variants and impact in global vaccination programs against SARS-CoV-2/COVID-19. Vaccines (Basel) 9, 243.

Hansen, J., Baum, A., Pascal, K.E., Russo, V., Giordano, S., Wloga, E., Fulton, B.O., Yan, Y., Koon, K., Patel, K., Chung, K.M., Hermann, A., Ullman, E., Cruz, J., Rafique, A., Huang, T., Fairhurst, J., Libertiny, C., Malbec, M., Lee, W.Y., Welsh, R., Farr, G., Pennington, S., Deshpande, D., Cheng, J., Watty, A., Bouffard, P., Babb, R., Levenkova, N., Chen, C., Zhang, B., Romero Hernandez, A., Saotome, K., Zhou, Y., Franklin, M., Sivapalasingam, S., Lye, D.C., Weston, S., Logue, J., Haupt, R., Frieman, M., Chen, G., Olson, W., Murphy, A.J., Stahl, N., Yancopoulos, G.D., Kyratsous, C.A., 2020. Studies in humanized mice and convalescent humans yield a SARS-CoV-2 antibody cocktail. Science 369, 1010–1014.

Harvey, W.T., Carabelli, A.M., Jackson, B., Gupta, R.K., Thomson, E.C., Harrison, E.M., Ludden, C., Reeve, R., Rambaut, A., Consortium, C.-G.U., Peacock, S.J., Robertson, D.L., 2021. SARS-CoV-2 variants, spike mutations and immune escape. Nat. Rev. Microbiol. 19, 409–424.

Hoffmann, M., Kleine-Weber, H., Schroeder, S., Kruger, N., Herrler, T., Erichsen, S., Schiergens, T.S., Herrler, G., Wu, N.H., Nitsche, A., Muller, M.A., Drosten, C., Pohlmann, S., 2020. SARS-CoV-2 cell entry depends on ACE2 and TMPRSS2 and is blocked by a clinically proven protease inhibitor. Cell 181, 271–280.

Huang, Y., Yang, C., Xu, X.F., Xu, W., Liu, S.W., 2020. Structural and functional properties of SARS-CoV-2 spike protein: potential antivirus drug development for COVID-19. Acta Pharmacol. Sin. 41, 1141–1149.

Hurt, A.C., Wheatley, A.K., 2021. Neutralizing antibody therapeutics for COVID-19. Viruses 13, 628.

Ju, B., Zhang, Q., Ge, J., Wang, R., Sun, J., Ge, X., Yu, J., Shan, S., Zhou, B., Song, S., Tang, X., Yu, J., Lan, J., Yuan, J., Wang, H., Zhao, J., Zhang, S., Wang, Y., Shi, X., Liu, L., Zhao, J., Wang, X., Zhang, Z., Zhang, L., 2020. Human neutralizing antibodies elicited by SARS-CoV-2 infection. Nature 584, 115–119.

Kim, C., Ryu, D.K., Lee, J., Kim, Y.I., Seo, J.M., Kim, Y.G., Jeong, J.H., Kim, M., Kim, J.I., Kim, P., Bae, J.S., Shim, E.Y., Lee, M.S., Kim, M.S., Noh, H., Park, G.S., Park, J.S., Son, D., An, Y., Lee, J.N., Kwon, K.S., Lee, J.Y., Lee, H., Yang, J.S., Kim, K.C., Kim, S. S., Woo, H.M., Kim, J.W., Park, M.S., Yu, K.M., Kim, S.M., Kim, E.H., Park, S.J., Jeong, S.T., Yu, C.H., Song, Y., Gu, S.H., Oh, H., Koo, B.S., Hong, J.J., Ryu, C.M., Park, W.B., Oh, M.D., Choi, Y.K., Lee, S.Y., 2021. A therapeutic neutralizing antibody targeting receptor binding domain of SARS-CoV-2 spike protein. Nat. Commun. 12, 288.

Lan, J., Ge, J., Yu, J., Shan, S., Zhou, H., Fan, S., Zhang, Q., Shi, X., Wang, Q., Zhang, L., Wang, X., 2020. Structure of the SARS-CoV-2 spike receptor-binding domain bound to the ACE2 receptor. Nature 581, 215–220.

Li, C.J., Huang, P.H., Chen, H.W., Chang, S.C., 2021. Development and characterization of mouse monoclonal antibodies targeting to distinct epitopes of Zika virus envelope protein for specific detection of Zika virus. Appl. Microbiol. Biotechnol. 105, 4663–4673.

Liu, L., Wang, P., Nair, M.S., Yu, J., Rapp, M., Wang, Q., Luo, Y., Chan, J.F., Sahi, V., Figueroa, A., Guo, X.V., Cerutti, G., Bimela, J., Gorman, J., Zhou, T., Chen, Z., Yuen, K.Y., Kwong, P.D., Sodroski, J.G., Yin, M.T., Sheng, Z., Huang, Y., Shapiro, L., Ho, D.D., 2020. Potent neutralizing antibodies against multiple epitopes on SARS-CoV-2 spike. Nature 584, 450–456.

Lu, R., Zhao, X., Li, J., Niu, P., Yang, B., Wu, H., Wang, W., Song, H., Huang, B., Zhu, N., Bi, Y., Ma, X., Zhan, F., Wang, L., Hu, T., Zhou, H., Hu, Z., Zhou, W., Zhao, L., Chen, J., Meng, Y., Wang, J., Lin, Y., Yuan, J., Xie, Z., Ma, J., Liu, W.J., Wang, D., Xu, W., Holmes, E.C., Gao, G.F., Wu, G., Chen, W., Shi, W., Tan, W., 2020. Genomic characterisation and epidemiology of 2019 novel coronavirus: implications for virus origins and receptor binding. Lancet 395, 565–574.

Min, L., Sun, Q., 2021. Antibodies and vaccines target RBD of SARS-CoV-2. Front Mol Biosci 8, 671633.

Pedelacq, J.D., Cabantous, S., Tran, T., Terwilliger, T.C., Waldo, G.S., 2006. Engineering and characterization of a superfolder green fluorescent protein. Nat. Biotechnol. 24, 79–88.

Shang, J., Ye, G., Shi, K., Wan, Y., Luo, C., Aihara, H., Geng, Q., Auerbach, A., Li, F., 2020. Structural basis of receptor recognition by SARS-CoV-2. Nature 581, 221–224.

Singh, J., Rahman, S.A., Ehtesham, N.Z., Hira, S., Hasnain, S.E., 2021. SARS-CoV-2 variants of concern are emerging in India. Nat. Med. 27, 1131–1133.

Tai, W., He, L., Zhang, X., Pu, J., Voronin, D., Jiang, S., Zhou, Y., Du, L., 2020. Characterization of the receptor-binding domain (RBD) of 2019 novel coronavirus: implication for development of RBD protein as a viral attachment inhibitor and vaccine. Cell. Mol. Immunol. 17, 613–620.

Wan, J., Xing, S., Ding, L., Wang, Y., Gu, C., Wu, Y., Rong, B., Li, C., Wang, S., Chen, K., He, C., Zhu, D., Yuan, S., Qiu, C., Zhao, C., Nie, L., Gao, Z., Jiao, J., Zhang, X., Wang, X., Ying, T., Wang, H., Xie, Y., Lu, Y., Xu, J., Lan, F., 2020. Human-IgG-neutralizing monoclonal antibodies block the SARS-CoV-2 infection. Cell Rep 32, 107918.

Wang, C., Li, W., Drabek, D., Okba, N.M.A., van Haperen, R., Osterhaus, A., van Kuppeveld, F.J.M., Haagmans, B.L., Grosveld, F., Bosch, B.J., 2020a. A human monoclonal antibody blocking SARS-CoV-2 infection. Nat. Commun. 11, 2251.

Wang, Q., Zhang, Y., Wu, L., Niu, S., Song, C., Zhang, Z., Lu, G., Qiao, C., Hu, Y., Yuen, K. Y., Wang, Q., Zhou, H., Yan, J., Qi, J., 2020b. Structural and functional basis of SARS-CoV-2 entry by using human ACE2. Cell 181, 894–904.

Wang, S., Peng, Y., Wang, R., Jiao, S., Wang, M., Huang, W., Shan, C., Jiang, W., Li, Z., Gu, C., Chen, B., Hu, X., Yao, Y., Min, J., Zhang, H., Chen, Y., Gao, G., Tang, P., Li, G., Wang, A., Wang, L., Zhang, J., Chen, S., Gui, X., Yuan, Z., Liu, D., 2020c. Characterization of neutralizing antibody with prophylactic and therapeutic efficacy against SARS-CoV-2 in rhesus monkeys. Nat. Commun. 11, 5752.

Wu, Y., Wang, F., Shen, C., Peng, W., Li, D., Zhao, C., Li, Z., Li, S., Bi, Y., Yang, Y., Gong, Y., Xiao, H., Fan, Z., Tan, S., Wu, G., Tan, W., Lu, X., Fan, C., Wang, Q., Liu, Y., Zhang, C., Qi, J., Gao, G.F., Gao, F., Liu, L., 2020. A noncompeting pair of human neutralizing antibodies block COVID-19 virus binding to its receptor ACE2. Science 368, 1274–1278.

Yan, R., Zhang, Y., Li, Y., Xia, L., Guo, Y., Zhou, Q., 2020. Structural basis for the recognition of SARS-CoV-2 by full-length human ACE2. Science 367, 1444–1448.

Yi, C., Sun, X., Ye, J., Ding, L., Liu, M., Yang, Z., Lu, X., Zhang, Y., Ma, L., Gu, W., Qu, A., Xu, J., Shi, Z., Ling, Z., Sun, B., 2020. Key residues of the receptor binding motif in the spike protein of SARS-CoV-2 that interact with ACE2 and neutralizing antibodies. Cell. Mol. Immunol. 17, 621–630.

Zheng, J., 2020. SARS-CoV-2: an emerging coronavirus that causes a global threat. Int. J. Biol. Sci. 16, 1678–1685.

Zhou, D., Dejnirattisai, W., Supasa, P., Liu, C., Mentzer, A.J., Ginn, H.M., Zhao, Y., Duyvesteyn, H.M.E., Tuekprakhon, A., Nutalai, R., Wang, B., Paesen, G.C., Lopez-Camacho, C., Slon-Campos, J., Hallis, B., Coombes, N., Bewley, K., Charlton, S., Walter, T.S., Skelly, D., Lumley, S.F., Dold, C., Levin, R., Dong, T., Pollard, A.J., Knight, J.C., Crook, D., Lambe, T., Clutterbuck, E., Bibi, S., Flaxman, A., Bittaye, M., Belij-Rammerstorfer, S., Gilbert, S., James, W., Carroll, M.W., Klenerman, P., Barnes, E., Dunachie, S.J., Fry, E.E., Mongkolsapaya, J., Ren, J., Stuart, D.I., Screaton, G.R., 2021a. Evidence of escape of SARS-CoV-2 variant B.1.351 from natural and vaccine-induced sera. Cell 184, 2348–2361.

Zhou, Y., Liu, Z., Li, S., Xu, W., Zhang, Q., Silva, I.T., Li, C., Wu, Y., Jiang, Q., Liu, Z., Wang, Q., Guo, Y., Wu, J., Gu, C., Cai, X., Qu, D., Mayer, C.T., Wang, X., Jiang, S., Ying, T., Yuan, Z., Xie, Y., Wen, Y., Lu, L., Wang, Q., 2021b. Enhancement versus neutralization by SARS-CoV-2 antibodies from a convalescent donor associates with distinct epitopes on the RBD. Cell Rep 34, 108699.

Zost, S.J., Gilchuk, P., Case, J.B., Binshtein, E., Chen, R.E., Nkolola, J.P., Schafer, A., Reidy, J.X., Trivette, A., Nargi, R.S., Sutton, R.E., Suryadevara, N., Martinez, D.R., Williamson, L.E., Chen, E.C., Jones, T., Day, S., Myers, L., Hassan, A.O., Kafai, N.M., Winkler, E.S., Fox, J.M., Shrihari, S., Mueller, B.K., Meiler, J., Chandrashekar, A., Mercado, N.B., Steinhardt, J.J., Ren, K., Loo, Y.M., Kallewaard, N.L., McCune, B.T., Keeler, S.P., Holtzman, M.J., Barouch, D.H., Gralinski, L.E., Baric, R.S., Thackray, L. B., Diamond, M.S., Carnahan, R.H., Crowe Jr., J.E., 2020. Potently neutralizing and protective human antibodies against SARS-CoV-2. Nature 584, 443–449.